Inverted ternary OPD based on PEIE

Tao An (antao@xaut.edu.cn)
Xi'an University of Technology https://orcid.org/0000-0002-9403-6578
Suiyang Liu
Xi'an University of Technology

Research Article

Keywords: OPD, Inverted, PEIE, Photoconductive

Posted Date: July 27th, 2021

DOI: https://doi.org/10.21203/rs.3.rs-667609/v1

Version of Record: A version of this preprint was published at Optical and Quantum Electronics on November 10th, 2021. See the published version at https://doi.org/10.1007/s11082-021-03344-6.

Noname manuscript No.
(will be inserted by the editor)

Inverted ternary OPD based on PEIE

Tao An · **Suiyang Liu**

Received: date / Accepted: date

Abstract This paper proposes an inverted ternary organic photodetector (OPD),whose structure is ITO/PEIE/$PC_{61}BM$/P3HT:PCPDTBT/MoO_3/Al. The use of PEIE as the cathode buffer layer avoids the influence of acidic PEDOT:PSS on the surface and life of the conventional device. The preparation of the ternary active layer ensures the photoelectric characteristics of the device in the visible-infrared broad spectrum range. In this experiment, the effect of PEIE thickness on the working mode of the device was studied by changing the concentration of the spin-coated PEIE solution. Finally, when the solution of PEIE is less than 0.45wt%, the device works in the diode mode, on the contrary, it works in the photoconductive mode. And under 550nm illumination(optical power 4.02mW/cm^2) , the device achieves a responsivity of 1.64A/W and an external quantum efficiency of 370%.

Keywords OPD · Inverted · PEIE · Photoconductive

1 Introduction

In recent years, OPD has gradually become a research hotspot, because it not only has the detection efficiency comparable to that of inorganic photodetectors, but also has the advantages of flexibility, diverse material choices, and simple manufacturing processes [1] [2] [3]. In the ternary OPD, based on the principle of spectrum broadening, three organic materials with complementary absorption peaks are used as the active layer to achieve detection in the full spectrum from ultraviolet to near-infrared [4] [5]. However, in the ternary OPD, there are still problems such as low external quantum efficiency and large dark current, and these problems seriously affect the detection efficiency of the device [6].

In order to solve the problem of the low external quantum efficiency of OPD, the researchers proposed that the device can be induced to produce a photoconductive effect by introducing traps [7]. This research group has conducted a lot of research on this, mainly focusing on doping electron traps to induce hole tunneling to improve the external quantum efficiency of the device. For example, the active layer P3HT: $PC_{61}BM$ is doped with C_{60} as an electron trap, so that the device can achieve an external quantum

Tao An
the School of Automation and Information Engineering, Xi'an University of Technique, Xi'an 710048, China.
Tel.: +189-66-888672
Fax: +123-45-678910
E-mail: antao@xaut.edu.cn

Suiyang Liu
the School of Automation and Information Engineering, Xi'an University of Technique, Xi'an 710048, China.

efficiency as high as 327.5 % under -1V bias voltage and 460nm illumination [8]. Doping C_{60} into the active layer PBDT-TT-F:$PC_{61}BM$, the device achieves an external quantum efficiency as high as 739.8% under a bias of -3V and 630nm illumination [9]. In order to solve the problem of low trap utilization in the case of high concentration single doping, this research group also proposed the use of double doping C_{60} and C_{70} to improve the trap utilization, and achieve 8 times the external quantum efficiency from 1067.48% to 8510.17% growth [10].Although the external quantum efficiency of the device can be significantly improved by doping traps in the active layer, there will be a phenomenon of doping gathered when doped with higher concentrations of doping, resulting in a reduction in the number of traps. It severely limits the practical application of trap-doped organic photomultiplier detectors.

Regarding the problem of large dark current in bulk heterojunction devices, the researchers proposed that devices with multiple active layer planar heterojunction structures can be fabricated. This approach can make the donor material and the acceptor material contact the anode and the cathode respectively, reducing the leakage current [11] [12] [13]. However, due to the short diffusion distance of free carriers in organic materials, it is necessary to make the active layer of the device thinner, resulting in insufficient absorption of the active layer and the problem of poor photoelectric properties of the device.

In order to solve the above problems, this paper uses PEIE as the cathode buffer layer to capture electrons at the cathode interface to induce hole tunneling injection to make the device work in the photoconductive mode to increase the external quantum efficiency. And in order to take into account the reduction of dark current and the increase of photocurrent, a composite structure of layered heterojunction and bulk heterojunction is adopted.

2 Experiment

2.1 Device preparation

An inverted ternary OPD was prepared in the experiment, and its structure was indium tin oxide (ITO)(20 mm×20 mm, 15Ω per square,Lumtec)/polyethoxyethyleneimine(PEIE)/$PC_{61}BM$/P3HT: PCPDTBT/MoO_3/Al. Figure 1 shows the structure diagram of the inverted ternary organic detector and the energy level diagram of the material. The PEIE buffer layer is prepared by diluting PEIE (80 % ethoxylated; 37 wt% in H_2O) solution with demineralized water to 0.15 wt%, 0.4 wt% and 0.45 wt%, and stir it with a magnetic stirrer at room temperature for 12 h. On the ITO that was cleaned with acetone and ethanol and dried with a nitrogen gun, spin-coated with a spin coater at a speed of 6000 rpm for 60 s, and then placed on a CNC heating plate for annealing for 30 min. The preparation of the acceptor active layer is to use an electronic balance to weigh 10 mg of $PC_{61}BM$ and dissolve in 1mL o-dichlorobenzene, and stir it fully with a magnetic stirrer at room temperature for 12 h. Then spin-coating on the PEIE buffer layer with a spin coater at 500 rpm for 60 s, and then annealed for 10 min. The donor active layer was prepared by weighing 7 mg of P3HT and 3 mg of PCPDTBT with an electronic balance, dissolving in 1 mL of o-dichlorobenzene, and fully stirring with a magnetic stirrer at room temperature for 12 h. Then spin-coating on the acceptor active layer with a magnetic stirrer at 500 rpm for 60 s, and then annealed for 10 min. The 15 nm MoO_3 electron blocking layer and the 100 nm anode Al were vapor-deposited using a high vacuum coater. Before the PEIE buffer layer is spin-coated, a part of ITO (5 mm×20 mm) needs to be etched away with concentrated hydrochloric acid as the area of the Al electrode. And shield a part of ITO (5 mm×20 mm) as the reserved cathode to avoid the contact between the anode and the cathode. The effective area of the final device is 1 cm^2.

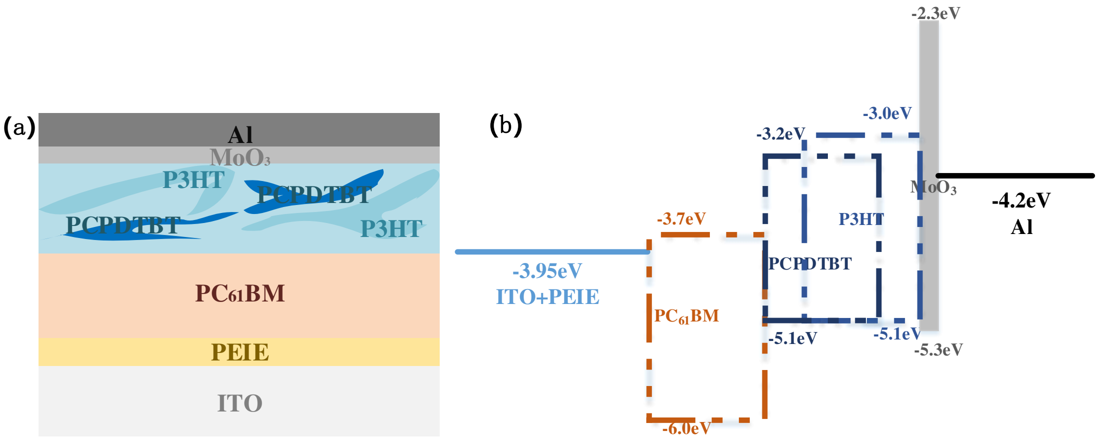

Fig. 1 (a) Structure diagram and (b) Energy level diagram of inverted ternary OPD

2.2 Testing and characterization

The Keithley 2636B Semiconducting System is used to test the J-V image to characterize the electrical characteristics of the device. The specific method is to connect the ITO cathode of the device to a high voltage, and the anode Al to a low voltage, and pass a direct current of -3V to 3V. Test the J-V of the device under different voltage driving and different wavelengths of light to the OPD. According to the electrical characteristics of the device, the external quantum efficiency (EQE), responsivity (R) and the specific detection rate (D^*) of the device can be obtained by calculation, and the performance of OPDs can be measured by these parameters. In order to directly understand the absorption of the OPD active layer film to different wavelengths of light, the UV-Vis spectrophotometer (PerkinElmer, Lambda 950) can be used to measure the absorbance of the active layer film of the device in the visible-infrared spectrum range.

2.3 Feature parameter calculation

The responsivity (R) , external quantum efficiency (EQE) and the specific detection rate (D^*) can be a good measure of the photoelectric characteristics of the device. The calculation formula is as follows:

$$R = \frac{J_{ph}}{P_{in}} = \frac{J_{light} - J_{dark}}{P_{in}} \tag{1}$$

$$EQE = J_{ph}hv/P_{in}q = Rhv/q = 1240 \cdot R/\lambda \tag{2}$$

$$D^* = \frac{R}{\sqrt{2qJ_{dark}}} \tag{3}$$

Among them, J_{ph} is the photogenerated current, which is equal to the difference between the photocurrent and the dark current, J_{light} is the current generated by the device under illumination, J_{dark} is the dark current, P_{in} is the incident light power and λ is the wavelength of the incident light.

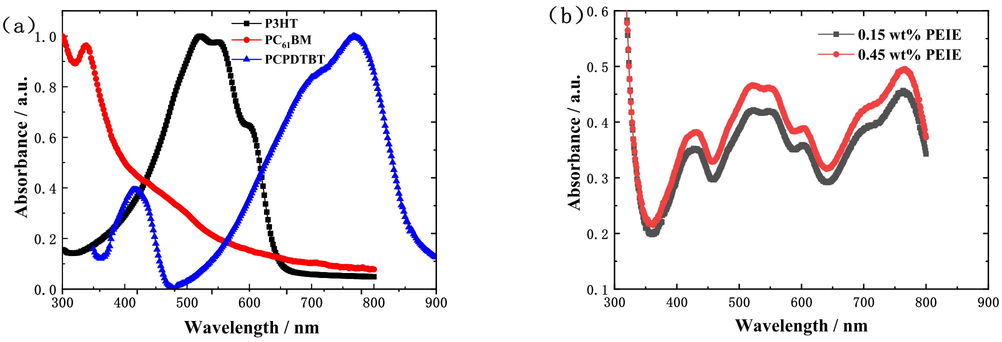

Fig. 2 (a) Absorption spectra of P3HT, PC_61BM and PCPDTBT films (b) Absorption spectra of ternary hybrid films on PEIE buffer layers with different thicknesses

3 Results and discussion

The test results of ternary OPDs with different PEIE thicknesses prepared in the experiment were analyzed, and spin-coated PEIE solution were 0.15 wt%, 0.4 wt% and 0.45 wt%. Through the test results of Abs spectrum and J-V to analyze the influence of different thickness of PEIE on the optical properties of the film and the electrical properties of OPDs. It is analyzed and concluded that the appropriate thickness of PEIE can effectively realize the high detection performance of the inverted ternary OPD in the visible light to near-infrared wavelength range.

In order to prepare inverted OPDs, this article focuses on the study of the effects of PEIE films of different thicknesses spin-coated with different mass ratios of PEIE solutions on the properties of OPDs. By measuring the absorption spectra of P3HT, $PC_{61}BM$ and PCPDTBT single material and mixed material films, as shown in Figure 2. As show by Figure 2, according to the principle of complementary absorption spectra, the ternary OPD proposed in this paper can achieve full-spectrum detection from visible light to near-infrared light [14]. And it is found that increasing the thickness of the PEIE film can increase the absorption intensity of the device in the full spectrum range. In order to explore the influence of different thicknesses of PEIE buffer layer films on the electrical characteristics of OPDs, the J-V characteristics of OPDs were tested under different optical powers of blue (460nm), green (530nm) and red (800nm). Figure 3 below shows the J-V diagram of the device under 0.15wt% PEIE solution spin-coated buffer layer and red light (800nm) with different optical powers. It can be concluded that under the irradiation of 800nm red light, its J-V characteristics tend to be the same regardless of its optical power. And its diode characteristics are not obvious compared with the buffer layer of OPDs spin-coated with 0.4wt% PEIE solution, and it is similar to a resistor with a fixed value. This is because the concentration of the spin-coated PEIE solution is too low and the thickness of the PEIE on the device is too thin to improve the energy level of the cathode ITO.

Figure 4 shows J-V characteristic curve of the OPDs spin-coated 0.4wt% PEIE solution as cathode buffer layer under green light (530nm) with optical power of 0.9, 1.45 and 3.3mW/cm^2 and red light (800nm) with optical power of 0.27, 0.65 and 1.23mW/cm^2.As shown in Figure 4, the photocurrent of OPDs spin-coated with 0.4wt% PEIE solution as a buffer layer under red light is an order of magnitude higher than that under green light. And no matter it is under the red light condition or the green light condition, the photocurrent will increase with the increase of the optical power under the bias voltage of 0-1v. This is because as the incident light power increases, the photogenerated excitons generated also increase, and the photocurrent by dissociation of the device will reach the reverse saturation current faster.

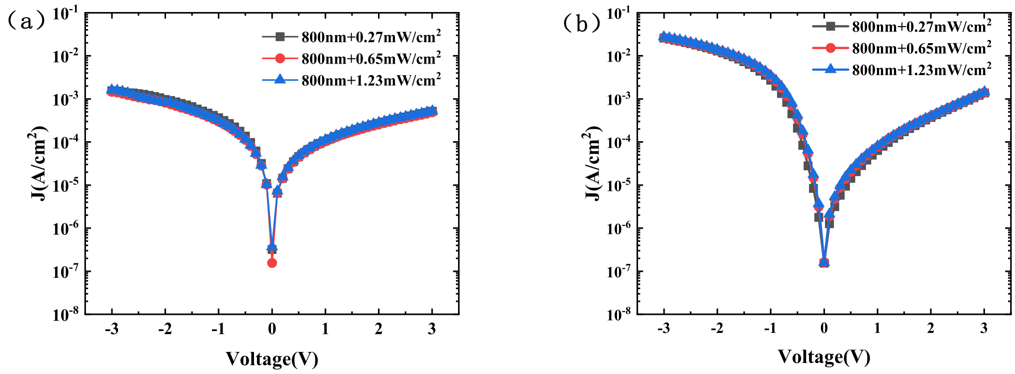

Fig. 3 J-V characteristic curve (a) 0.15wt% (b) 0.4wt% PEIE solution as the buffer layer of OPDs

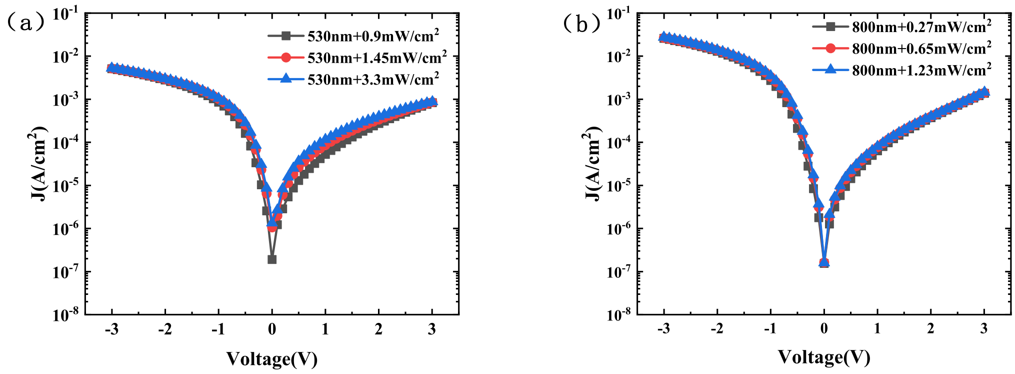

Fig. 4 J-V characteristic curve of OPDs with 0.4wt% PEIE solution as buffer layer (a) under green light (b) under red light

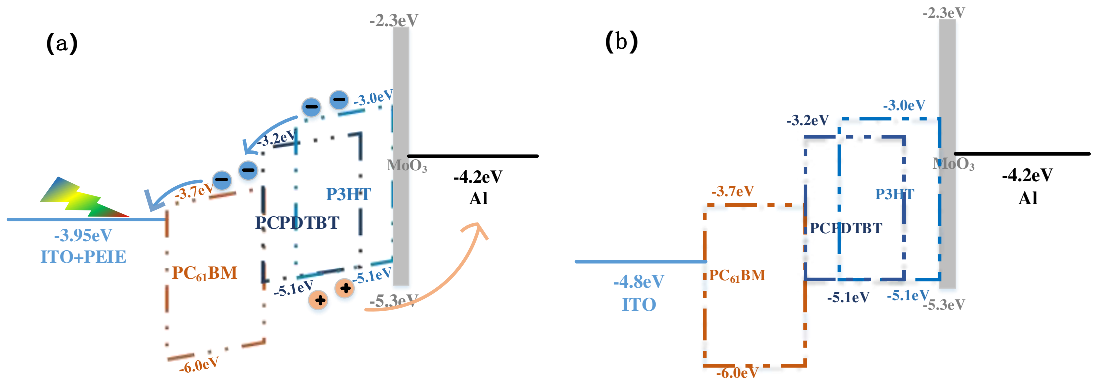

Fig. 5 (a) Working principle diagram of inverted OPDs (b) Energy level diagram of devices without spin-coated PEIE

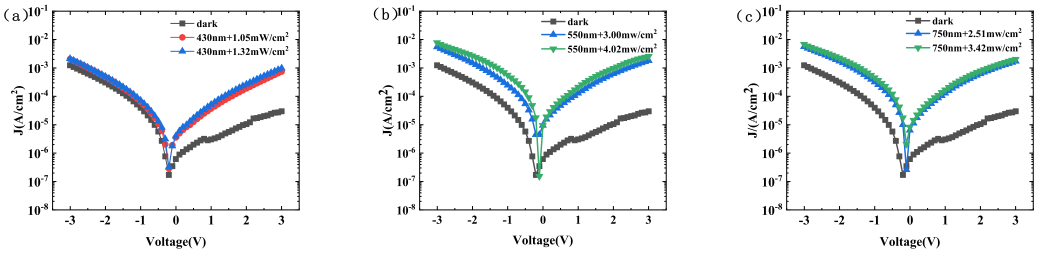

Fig. 6 J-V plot of three-phase inverted OPDs spin-coated 0.45wt% PEIE solution (a) under dark conditions and 430nm light (b) under dark conditions and 550nm light (c) under dark conditions and 750nm light

Table 1 R and EQE of OPDs at a bias voltage of 2.5V and placed under different light conditions.

Lighting conditions	R(A/W)	EQE(%)	D*(Jones)
430nm+1.05mW/cm^2	0.71	203	2.798*10^{11}
430nm+1.32mW/cm^2	0.98	281	3.862*10^{11}
550nm+3.01mW/cm^2	1.04	233	4.099*10^{11}
550nm+4.02mW/cm^2	1.64	370	6.463*10^{11}
750nm+2.51mW/cm^2	1.00	225	3.941*10^{11}
750nm+3.42mW/cm^2	1.23	278	4.847*10^{11}

Figure 5 shows the working principle diagram of inverted OPDs. The energy level of ITO itself is -4.8eV, and the energy level of ITO is increased to -3.95eV by spin coating with a suitable thickness of PEIE [15][16]. If the PEIE spin-coated is too thin, ITO will be closer to the HOMO energy level of $PC_{61}BM$, and it will tend to be an anode that collects holes rather than a cathode that collects electrons. However, due to the presence of the MoO_3 electron blocking layer in the inverted device [17], the device cannot be an conventional OPDs. Therefore, the J-V curve of the OPDs device that spin-coated 0.15wt% PEIE solution as a buffer layer does not show obvious diode characteristics.

Figure 6 below is the J-V plot of three-phase inverted OPDs spin-coated with 0.45wt% PEIE solution under dark conditions and 430n, 550nm, 750nm light.

EQE, R and D* of OPDs can be calculated according to formula (1), (2),(3) and the value of J-V curve. Under a bias of 2.5V, the R and EQE of the three-phase inverted OPDs spin-coated 0.45wt% PEIE solution under different illumination and different optical power are shown in Table 1 below.

It is obvious from Table 1 that the R, EQE and D* of the device are highly dependent on the light intensity. In the case of the same wavelength, R and EQE increase with the increase of the light intensity, but in the case of different wavelengths, the light intensity is not the main factor affecting the R and EQE of the device. For example, the external quantum efficiency under blue light conditions of 430nm and 1.32mW/cm^2 is much higher than that under red light conditions of 750nm and 2.51mW/cm^2. This phenomenon can be explained as a decrease in the trapping efficiency of additional excitons generated by the increase in optical power due to the saturation of electron traps and the decrease in induced hole mobility. It can be seen from Table 1 that the EQE of the device is greater than 100%, which indicates that the device has a photoconductivity effect [18][19]. This is because the spin-coated PEIE buffer layer increases the energy level of ITO [20]. The higher energy barrier will cause the accumulation of photogenerated electrons at the interface between PEIE and the active layer, thereby greatly increasing the photocurrent gain, making EQE>100%. The specific working mechanism of the OPDs photomultiplier caused by the PEIE buffer layer is shown in Figure 7 below. When the device is exposed to light, the excitons generated by the absorption of photons by the active layer $PC_{61}BM$ and P3HT:PCPDTBT film will dissociate at the interface of the $PC_{61}BM$ and P3HT:PCPDTBT film. The holes generated by

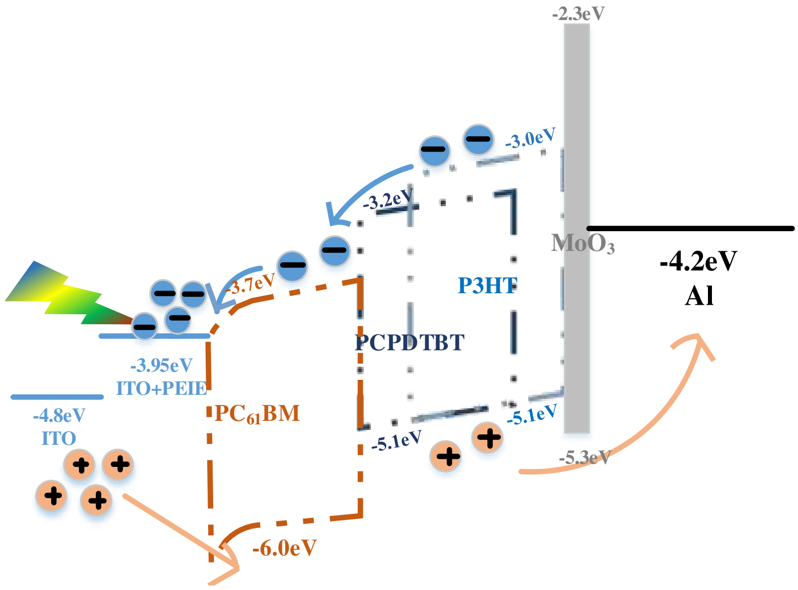

Fig. 7 The working mechanism of OPDs photomultiplier caused by PEIE buffer layer

dissociation move to the HOMO energy level of P3HT:PCPDTBT and the electrons move to the LOMO energy level of $PC_{61}BM$. In the inverted device, because the PEIE-modified ITO has an increased barrier at the interface of the active layer, a more effective interface photoelectron capture is achieved. This high-strength bound electrons will thin the barrier for hole injection from the ITO electrode, and at the same time further lead to hole injection from ITO to P3HT. When a reverse bias is applied to the device, even under very low light intensity, the accumulation of electrons at the interface between the active layer and the electrode will induce tunneling and injection of holes on the electrode, resulting in a higher photocurrent.

4 Conclusion

In a word, this paper designs an inverted OPD whose structure is ITO/PEIE/$PC_{61}BM$/P3HT: PCPDTBT/MoO_3/Al. Among them, the PEIE buffer layer makes the device work in the photoconductive mode, and three different active layer materials make the device work in the full spectrum range. Among them, when 0.45wt% PEIE solution is spin-coated, under 550nm light and the optical power is 4.02mW/cm^2, the device achieves a responsivity of up to 1.64A/W and an external quantum efficiency of 370% under 2.5V bias.

References

1. Jansen-Van Vuuren R D, Organic Photodiodes: The Future of Full Color Detection and Image Sensing, Advanced Materials, 28, 4766-4802(2016).
2. Sunniya Iftikhar,Saba Aslam,Prato reaction derived polythionphene/C_{60} donor-acceptor double cable polymer,fabrication of photodetectors and evaluation of photocurrent generation,Journal of Mateials Chemistry C,8,17365-17373(2020).
3. Zang D,Huang C,A Di, et al, Device engineered organic transistors for flexible sensing applications, Advanced Materials,28,4549-4555(2016).
4. W Li, Y Xu Lin,Visible to near-infrared photodetection based on ternary organic heterojunctions, Advanced Functional Materials,29, 1808948(2019).

5. Hanyu Wang,Yifan Zheng,Highly sensitive panchromatic ternary polymer photodetectors enabled by Förster resonance energy transfer and post solvent treatment,Journal of Physics D: Applied Physics,51,104002(2018).
6. S. Valouch, C, Solution processed small molecule organic interfacial layers for low dark current polymer photodiodes ,Organic Electronics,13,2727-2732(2012).
7. Li, Lingliang and Zhang, Fujun,Trap-Assisted Photomultiplication Polymer Photodetectors Obtaining an External Quantum Efficiency of 37500% ,ACS Applied Materials & Interfaces,7,890-5897,(2015).
8. Wei Gong,Tao An,Xinying Liu,and Gang Lu,Realizing photomultiplication-type organic photodetectors based on C_{60}-doped bulk heterojunction structure at low bias,Chinese Physics B,28,038501(2019).
9. Tao An,Wei Gong,Jianping Ma,Photoelectronic multiplication organic photodetectors with facile fabrication and controllable operating voltage,Organic Electronics,67,320-326(2019).
10. Tao An,Xinying Liu,Jianping Ma,A new method to enhance organic photodetectors active layer trap doping by blending doping,Semiconductor Science and Technology,35,1-5,(2020).
11. S.Shafian,Y.Jang and K.Kim,Solution processd organic photodetector ultizing an interdiffused polymer/fullerene bilayer, Optics Express,15,A936-A946(2015).
12. D.Z.Yang,X.K.Zhou,Fast response organic photodetectors with high detectivity based on rubrene and C_{60},Organic Electronics,14,3019- 3023(2013).
13. D.Yang,K.Xu,Comprehensive studies of response characteristics of organic photodetectors based on rubene and C_{60}, Applied Physics,115,244506(2014).
14. Shen, Liang and Zhang, Yang,A filterless, visible-blind,narrow-band, and near-infrared photodetector with a gain,Nanoscale,8,12990-12997,(2016).
15. Yue Wang,Lijie Zhu,High sensitivity and fast response solution processed polyethylenimine ethoxylated(PEIE) modified ITO electrode,Research Article Optics Express,25,7719-7729,(2017).
16. Tomasz Klab,Beata Luszczynska,Influence of PEIE inter-layer on detectivity of red-light sensitive organic non-fullerene photodetectors with reserve structure,Organic Electronics,77,105527(2020).
17. Li Yi,Chen Hu,Carrier Blocking Layer Materials and Application in Organic Photodetectors, Nanomaterials,11,1404,2021.
18. Liu MengYao,Wang Jian,Broadband Photomultiplication organic photodetectors,Physical Chemistry Chemical Physics,23,2923-2929(2021).
19. Kublitski Jonas,Hofacker Andreas,Revers dark current in organic photodetectors and the major role of traps as source of noise,Nature Communications,12,1-9(2021).
20. Ikram Anefnaf,Safae Aazou,Tailoring PEIE capped ZnO binary cathode for solution-processed inverted organic solar cells,Optical Materials,116,111070(2021).